Hydrophilic Polymers for Biomedical Applications:

In 2000, our group was funded by a local industry, Benz R&D and the State of Florida. The task at hand was to develop an understanding of water structure in crosslinked, hydrophilic polymers and copolymers containing 2,3-dihydroxypropyl methacrylate (DHPMA)and 2-hydroxyethyl methacrylate (HEMA). Benz R&D wanted to prove superior performance in their DHPMA contact lens formulations. This work led to a collaboration with Dr. Moussy in the Biomedical Engineering Department at USF. <u>NIH funded us for 5 years (2004-2009) to research glucose sensor tissue interactions</u>. Our laboratory is responsible for identifying rugged, biocompatible, hydrophilic sensor coatings. We continue to probe the polymer structures to increase our knowledge of water structure and relaxation behavior in these polymers and highlight some of our findings below.

We investigated water structure in PHEMA, PDHPMA and two copolymers with 1 to 1 and 3 to 1 HEMA to DHPMA molar ratios, using samples equilibrated in water at 20°C (30-32). The equilibrium water content increased from 38 wt % in PHEMA to 75 wt % in PDHPMA. Water in hydrogels is classified as free (freezing) and bound water; bound water exits as freezing-bound water and nonfreezing-bound water (33). In DSC studies, freezing water exhibits a crystallization exotherm at about -20°C, where as freezing bound water associated with the matrix exhibits an exotherm at about -40 °C (34). Nonfreezing water molecules are tightly associated with the hydrophilic groups on the polymer and cannot be detected by DSC. Nonfreezing water is, however, calculated from the intercept of plots of total exotherm area versus water content. We determined that in HEMA, the majority of the water is nonfreezing bound water, about 35 wt %. This agrees with previous amounts determined by DSC and NMR, 30±5 wt% (34). Small amounts of DHPMA when co polymerized with HEMA increase the freezing, freezing bound and nonfreezing water content. PDHPMA homopolymer exhibits a single exotherm at around -20°C; all of the water is either free water or nonfreezing-bound water. When PDHMA samples are desorbed to various degrees, the crystallization exotherms vanish at 43 wt%.

The enhanced water content of the PDHPMA gels enticed us to characterize desorption kinetics from 16-37°C in samples equilibrated at 30% and 60% relative humidity. We conducted the first study that we are aware of that focuses on the initial drying period, critical to contact lens applications, and during which initial weight loss data is proportional to time; boundary layer phenomenon control evaporation. The details of these intricate experiments are given in ref. 32. The main objective was to determine the effect of the extra hydroxyl group in DHPMA on water desorption. We did observe that the extra hydroxyl group slowed the evaporation process and that DHPMA containing polymers exhibited higher activation energies for volatility than HEMA homopolymer.

Dynamic mechanical analysis studies conducted during desorption revealed that polymers increased in stiffness as materials desorb (fig. 7). The stiffness increase was greatly accelerated in HEMA containing polymers and this effect decreased with increasing DHPMA
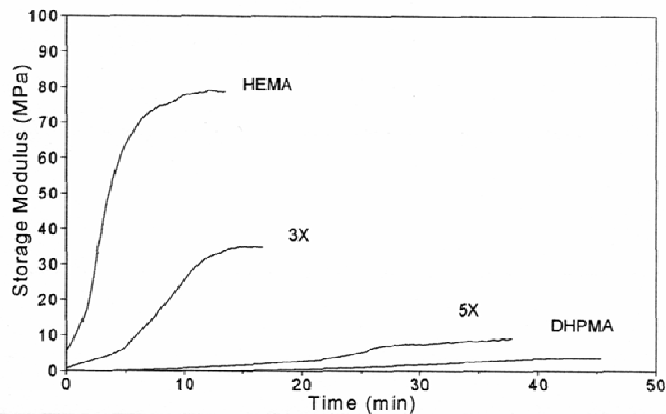
Figure 7

DHPMA homopolymer showed no change until the sample desorbed 15 minutes at 23 °C. This retention of water and modulus induced by the extra hydroxyl group directly relates to the enhanced performance of these contact lens materials. Further, we conducted initial ion transport studies on 1:1 mole ration copolymer and PHEMA. We demonstrated accelerated Na^+ and K^+ transport rates in the copolymer.

We analyzed dynamic mechanical relaxations in these polymers in the xerogel (dry) state and at various states of hydration (31). Whereas, PHEMA relaxation behavior has been characterized in the xerogel state and at low levels of hydration (35), DHPMA and HEMA/DHPMA copolymers have not been extensively studied. The aim was to focus on secondary relaxations in these systems. Such relaxations that occur in glassy polymer below the glass transition temperature are the result of four types of molecular motion (36). These are: motion of short chain segments in the backbone, rotation of side groups attached to the backbone, internal motion within a side group and motion of, or within small molecules dissolved in the matrix. In xerogel form, HEMA exhibits a primary, α relaxation associated with glass transition, a β relaxation associated with rotations of the carbonyl side group and a γ transition due to internal motion of the hydroxyl group on the side chain. Upon hydration of HEMA a new secondary transition occurs, the β_{sw} transition, at temperatures above the γ transition. This transition is due to the forth type of motion and consists of water molecules interacting with hydroxyalkyl group on the side chain (35).

In xerogel DMA data, the β relaxation was obscured by overlap with the α transition PHEMA and PHEMA/DHPMA copolymers. The β transition was clearly more pronounced in the DHPMA xerogel and the apparent activation energy was 32 kcal/mol. The γ transition temperature increased with increasing DHPMA content from -132°C in HEMA homopolymer to -96° C in
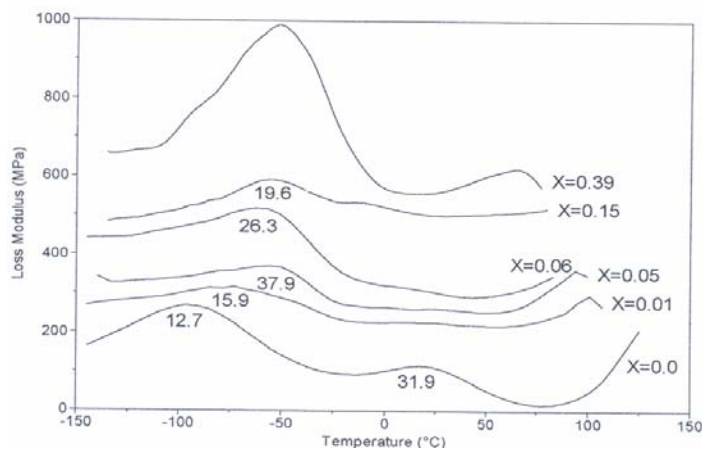

Figure 8

PDHEMA. Similarly the apparent activation energies increased in the order HEMA = 7.5 kcal/mol, 1DHPMA/3HEMA = 11.5 kcal/mol, 1DHPMA/!HEMA = 11.8 kcal/mol and DHPMA = 12.7 kcal/mol. All of this reflects greater interaction due to the extra hydroxyl group on the side chain in DHPMA.

During initial hydration, the intensity of the γ transition in all samples gradually decreased while the temperature remained constant for a given frequency. At the same time, the β_{sw} transition formed at higher temperatures. It decreased in temperature and increased in intensity at the expense of the γ transition (fig.8). Again, the temperature maxima of both transitions and the activation energies increased with DHPMA content. These results concurred with initial dielectric data.

While the dielectric response of sub T_g relaxations in HEMA and HEMA/DHPMA copolymers has been studied, there is no data above 50°C. This is due to the fact that conductivity effects obscure relaxations, even in xerogels. The first aim of this research was to focus on PHEMA and then to extend the study to include the DHPMA materials and nanocomposite materials.
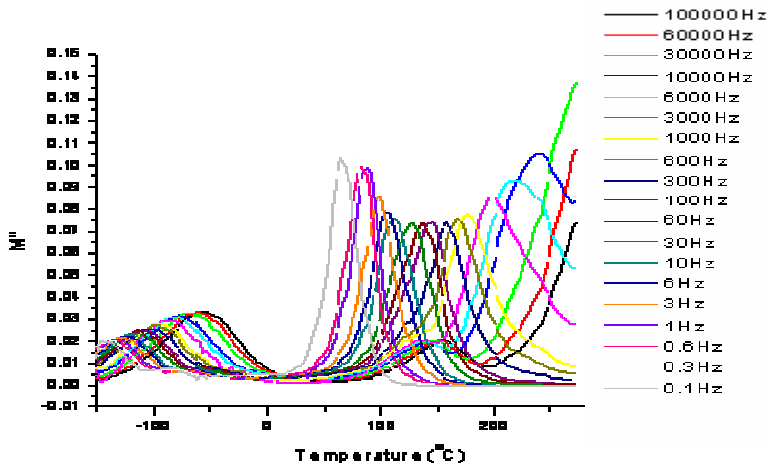

Figure 9: A plot of M" versus temperature for a range of frequencies for the neat PHEMA zerogel.

The dielectric permittivity, ε', and the loss factor, ε", of dry poly(2-hydroxyethyl methacrylate) (PHEMA) were measured using a dielectric analyzer (DEA) in the frequency range of 0.1Hz to 100 kHz and between the temperature range of -150 ºC to 275 ºC (37) Three different processes were observed at 50 ºC and above. Due to the paucity of DEA data in literature covering this temperature range we set out to decipher the meaning of the dielectric spectra of dry PHEMA. The electric modulus formalism was used to reveal the γ, β, α (αβ merge) and conductivity relaxations present in this polymer (37,38,39). This study is important because dielectric behavior gives insight into not only the structural property and relaxations present in the polymer but can also be used to investigate the conductivity and interaction of the polymer systems containing nanofillers. Using the electric modulus formalism we were able to differentiate between the viscoelastic relaxations in the polymer and the conductivity relaxation which occurs as a result of bulk ionic conduction.

The complex electric modulus, M^*, is made up of real (M') and imaginary (M'') electric modulus components which are shown in the equation below.

$$M^* = \frac{1}{\varepsilon^*} = M' + iM'' = \frac{\varepsilon'}{\varepsilon'^2 + \varepsilon''^2} + i\frac{\varepsilon''}{\varepsilon'^2 + \varepsilon''^2}$$

Three mathematical approaches were used to accomplish this task.

Approach #1: Argand plots (*M''* vs. *M'*) of the components of the complex modulus, *M**, were generated. We demonstrated that the conductivity relaxation exhibits true semi-circular behavior in accordance with the equation given below; whereas in the viscoelastic region, Argand plots deviate from semi-circular behavior. Semi-circular behavior is characteristic of the Debye model, in particular molecular liquids and small rigid molecules; conductivity relaxations in ionic conductors have been found to also exhibit single relaxation times (38,40,41). Polymers, on the other hand, deviate from semicircular behavior in which they exhibit a distribution of relaxation times and are often characterized by modified Argand expressions.

$$\left\{M' - \frac{(M_U + M_R)}{2}\right\}^2 + (M'')^2 = \left(\frac{M_U - M_R}{2}\right)^2$$

Approach #2: An expression for the electric modulus (*M*) was previously formulated by Ambrus et. al. (38,42), assuming that ionic conduction is purely due to the diffusion of ions and independent of any viscoelastic, dipolar relaxation. This assumption implies that the electric modulus (*M*) will exhibit a single relaxation time, τ_σ. Additionally, plots of log [*M'*] and log [*M''*] vs. log frequency exhibit slopes of 1 and 2, respectively. As expected our plots reveal slopes of 1 and 2 at temperatures in the region of the conductivity relaxation. Similar plots were not obtained for temperatures in the glass transition region and below.

$$M = Ms(\frac{i\omega\tau_\sigma}{1 + i\omega\tau_\sigma}) = M_s\left[\frac{(\omega\tau_\sigma)^2}{1 + (\omega\tau_\sigma)^2}\right] + iM_s\left[\frac{\omega\tau_\sigma}{1 + (\omega\tau_\sigma)^2}\right]$$

Approach #3: Two processes contribute to the dielectric loss factor. When viscoelastic effects are negligible, the loss factor is described by the ionic conductivity given by the equation: $\sigma_{ac} = \varepsilon''\omega\varepsilon_o$. We obtained dc conductivity (σ_{dc}) by extrapolating to zero frequency, and determined the temperature dependence of the dc conductivity. We found that the ionic conductivity peak from the electric modulus plot yielded the same temperature dependence and activation energy as the dc conductivity. This further verified that the particular region in the dielectric spectrum in question was in fact due to conductivity and not viscoelastic contribution from the polymer (43,44). We are currently extending this analysis to other hydrogel systems.

Biocompatability studies: Interactive Surface Hydrogels as Biocompatible Coatings for Implantable Glucose Sensors.

Our objective is to formulate, modify and characterize a biocompatible coating for an implanted glucose sensor device. This coating should:

1. be permeable to allow glucose, oxygen and hydrogen peroxide to diffuse freely,
2. reduce adsorption of protein from surrounding cell and plasma,
3. result in minimal fibrosis by having an interface that is compatible with the tissue.
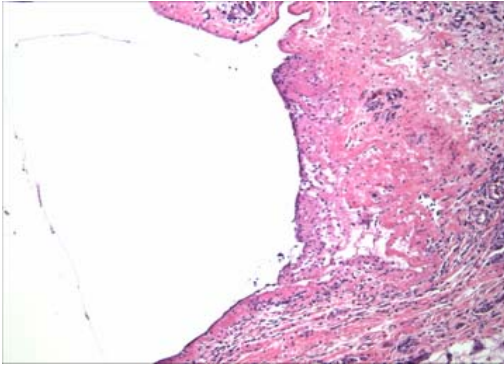

Figure 10: 80:20 molar ratio HEMA-DHPMA hydrogel exhibiting almost no fibrosis after 28 days of implantation.

This biocompatible coating will effectively be a hydrogel. Certain hydrogels, due to their high biocompatibility, have been used in the biomedical field as materials for contact lens, artificial tissue engineering, bioadhesives, and implantable devices, such as controlled release drug delivery systems. Random block copolymers of 2-hydroxyethyl methacrylate (HEMA) and 2,3-dihydroxypropyl methacrylate (DHPMA) cross-linked with ethylene glycol dimethacrylate have been synthesized in a series of various molar ratios. Various tests have been performed to determine hydrogel stability and equilibrium water content in buffered saline solution. Other mechanical and thermal tests are underway. Dr. Moussey undertook animal testing of the hydrogels and we obtained encouraging results in which particular formulations exhibited minimal to no fibrosis at the implant site (fig. 10). Our laboratory is now in the process of coating active sensors with the hydrogels using various coating techniques such as plasma polymerization and dip coating.

References

30 "Water Structure in Hydroxyethyl-Co-Glycerol Methacrylate Materials", G. Gates, J. P. Harmon, J. Ors and P.Benz, <u>ANTEC</u> 59th Vol. 2, 1898 (2001).

31 "Intra and Intermolecular Relaxations in 2,3-Dihydroxypropyl and 2-Hydroxyethyl Methacrylate Hydrogels", <u>Polymer</u>, Vol. 44, 207 (2003).

32 "2,3-Dihydroxypropoyl Methacrylate and 2- Hydroxyethyl Mehtacrylate Hydrogels: Gel Structure and Transport Properties", <u>Polymer</u>, Vol. 44, 215 (2003).

33 "Interaction Between Water and Hydrophilic Polymers", H. Hatakeyama and T. Hatakeyama, <u>Thermochimica ACTA</u>, 308, 3 (1998).

34 "Water in Hydrogels. 1. A Study of Water in Poly(N-vinyl-2-pyrrolidone/methyl methacrylate) Copolymer", F. Quinn, E. Kampff, G. Smyth, and V. J. McBrierty, <u>Macromolecules</u>, Vol. 21, 3191 (1988).

35 "Mechanical Behavior of Hydroxyalkyl Methacrylate Polymers and Copolymers", J. Janacek, <u>Reviews in Macromolecular Chemistry</u>, Vol. 10, 1, (1973).

36 "Molecular Origin of relaxations in Polymers", J. Heijboer, <u>In Molecular Basis of Transitions and Relaxations</u>, New York: Gordon and Breach Science Publishers Press, 75 (1978).

37 "A Broad Spectrum Analysis of the Dielectric Properties of Poly (2-hydroxyethyl methacrylate", K. Mohomed, T. G. Gerasimov, F. Moussy and J. P. Harmon, <u>Polymer</u>, Vol. 46, 3847 (2005).

38 "Conductivity Relaxation in a Concentrated Aqueous Electrolyte Solution", J.H. Ambrus , C.T. Moynihan, P.B. Macedo, <u>Journal of Physical Chemistry</u>, Vol. 76(22), 3287-3295 (1972).

39 <u>Anelastic and Dielectric Effects in Polymeric Solids</u>, N.G. McCrum, B.E. Read, G. Williams, and New York: Dover, (1967).

40 "The Dipolar and Conductivity Relaxations in Ionic Conductors" G.P. Johari, K. Pathmanathan, <u>Physical Chemistry of Glasses</u>, Vol. 29(6), 219-224 (1988).

41 "The Merging of the Dielectric α- and β-relaxations in Poly-(Methyl Methacrylate)", R. Bergman, F. Alvarez, A. Alegria, J. Colmenero, <u>Journal of Chemical Physics</u>, 109(17), 7546 (1998).

42 "Dielectric Analysis of Polymers" P. Avakian, H.W. Starkweather, Jr., W.G. Kampert, S.Z.D. Cheng, editor. <u>Handbook of Thermal Analysis and Calorimetry</u>, New York: Elsevier, Vol. 3, pp. 147-164 (2002).

43 "Electrical Conductivity Studies in Hydrogels" P. Pissis, A. Kyritsis, Solid State Ionics, Vol. 97, 105-113 (1997).

44 "Structure-property Relationships in Proton Conductors Based on Polyurethanes", P. Pissis, A. Kyritsis, G. Georgoussis, V.V. Shilov, V.V. Shevchenko, <u>Solid State Ionics</u>, Vol. 136-137, 255-260 (2000).